

THE EFFECT OF Ag PRECIPITATES ON STRENGTH AND DUCTILITY OF CuAgZr ALLOY

Waraporn Piyawit^{1,*}, and Panya Buahombura²

Received: August 22, 2017; Revised: October 25, 2017; Accepted: November 6, 2017

Abstract

CuAgZr alloy is remarkably well-known for a good compromise between high strength and high electrical conductivity. The strength is mainly contributed by the self-aligned nanosized Ag precipitates on {111} planes in the Cu matrix. In this study, the evolution of Ag precipitates in Cu-7wt%Ag-0.05wt%Zr during thermal processing was characterized to control the alloy microstructures in order to improve the mechanical strength and electrical conductivity. The solution-treated CuAgZr alloy samples were cold rolled with a logarithmic strain of 2.3 and subsequently aged for various times. The X-ray diffraction and electron microscopy techniques indicate the evolution of precipitate size distribution during different thermal routines and clarify that the change of dislocation density has a direct effect on Ag precipitation behavior and distributions. This paper discusses the correlation between the effect of plastic deformation and the evolution of nanoscale Ag precipitates, which provides the strength and electrical conductivity of this alloy.

Keywords: Copper alloy, plastic deformation, precipitates, strengthening

Introduction

Copper and its alloys are widely used in various electrical and electronics applications because of their decent electrical conductivity. Nevertheless, copper is 1 of the metals that have high specific gravity. In order to reduce the size and weight of applications, copper needs to be stronger to achieve higher specific strength. However, a work hardening

mechanism can significantly lower the electrical conductivity and workability of the materials. CuAgZr alloy has been remarkably recognized as a high strength and high conductivity copper alloy (Hirota *et al.*, 1994; Gaganov *et al.*, 2006; Lyubimova *et al.*, 2010; Monzen *et al.*, 2010). This alloy can be strengthened along with an increasing

¹ School of Metallurgical Engineering, Suranaree University of Technology, Nakhon Ratchasima 30000, Thailand. E-mail: wpiyawit@sut.ac.th

* Corresponding author

electrical conductivity through a precipitation hardening process (Hanama *et al.*, 2011; Bao *et al.*, 2016). The precipitation mechanism in Cu-7wt%Ag-0.05wt%Zr has been characterized by high resolution transmission electron microscope (TEM) in a previous study (Piyawit *et al.*, 2014). It was suggested that Ag precipitates were formed by clustering of the Ag atoms faceted on {111} planes of Cu matrix and maintained a cube-on-cube orientational relationship with the matrix. Precipitate formation on particular {111} planes can be described by the minimization of energy. The thickening of nanoscale Ag precipitates appears to be by the ledge growth mechanism. Piyawit *et al.* (2014) suggested that this is a result of misfit dislocation networks on the Ag-Cu interface. The high performance of Cu base alloys can be achieved by the fine precipitates formed in the Cu matrix during the aging process. However, the in-depth analysis of Ag precipitation behaviors affected by deformation strain due to plastic deformation has not been thoroughly clarified. In order to successfully gain a good compromise between the strength and electrical conductivity, it is important to understand the effects of precipitates on the mechanical behavior of the alloy. The tailoring of the Ag precipitation in the Cu matrix can provide these desirable properties.

In this study, the plastically deformed CuAgZr alloy with a logarithmic strain of 2.3 will be characterized by X-ray diffraction, electron microscopy, and mechanical testing in order to clarify the effects of precipitation on the microstructure, tensile properties, and fracture behavior of Cu-7wt%Ag-0.05wt%Zr alloy.

Materials and Method

The alloy that was examined in this work was a Cu-7wt%Ag-0.05wt%Zr, which has good strength and good electrical conductivity. The details of the alloy preparation is described elsewhere (Piyawit, 2014). Cylindrical cast samples with 10 mm diameters were cut into disks with a thickness of 3 mm and solution

treated at 850°C for 5 h in a tube furnace with a controlled argon atmosphere followed by water quenching. The solution-treated samples were subsequently rolled by the logarithmic strain of 2.3 at room temperature (denoted as the CR sample). A schematic illustration of the sample preparation is shown in Figure 1. The deformed samples were isothermally heat treated at 430°C with different aging times. The X-ray diffraction (XRD) measurement was performed using a conventional X-ray diffractometer (D8 ADVANCE, Bruker AXS GmbH, Karlsruhe, Germany). Diffraction profiles were measured in Bragg-Brentano geometry ($2\theta-\theta$) utilizing Cu $K\alpha$ radiation. Dog-bone shaped tensile specimens for uniaxial tensile tests were cut from the deformed samples with gauge lengths of 10 mm, a width of 1 mm, and a thickness of 250 ± 30 μm along the rolling direction, as shown in Figure 1 and tested on an Instron 5565 servo hydraulic testing machine (Instron Corp., Norwood, MA, USA) with a 5 kN load cell with a cross head velocity of 1 mm/min. The tensile tests were carried out for each process condition 3 times. The measurement of the electrical conductivity was carried out using the four-point-probe method that has been described elsewhere (Bowler and Huang, 2005).

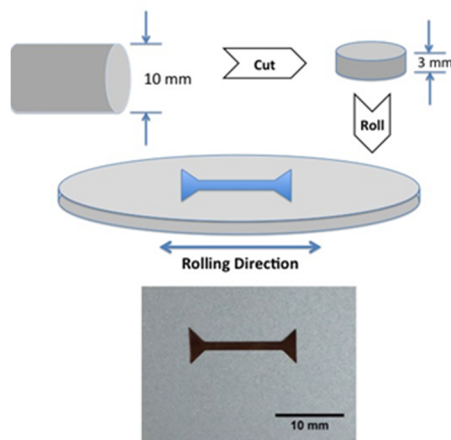


Figure 1. Schematic illustration and image of tensile specimen preparation

As-rolled and aged samples were polished and etched in a solution of 100 ml H₂O, 50 ml HCl, and 5 g FeCl₃. Scanning electron microscopy (SEM) of the aged samples was done with the Auriga series (Carl Zeiss AG, Oberkochen, Germany) at 6 kV. SEM examination at a low accelerating voltage benefits the surface investigation. The average size of the Ag precipitates can be measured from SEM micrographs using the ImageJ program. The fractography examinations of the tensile specimens were carried out using a JEOL6010-LV scanning electron microscope (JEOL Ltd., Tokyo, Japan). The accelerating voltage used during examination was 20 kV. Specimens for the TEM were prepared by the Gatan PIPS system for ion milling (Gatan, Inc., Pleasanton, CA, USA) using 3 keV. The TEM characterizations were performed using a JEOL JEM-2000FX (JEOL, Ltd., Tokyo, Japan). The microscope was operated at 200 kV.

Results and Discussion

X-Ray Diffraction

X-ray diffraction (XRD) patterns of the deformed samples which examined the composition and structural evolution during different thermal routines are shown in Figure 2. The reference patterns used in the analysis were PDF# 85-1326 for copper, 87-0720 for silver, 03-0884 for CuO, and 05-0667 for Cu₂O, respectively. The cold rolled sample without thermal treatment, denoted as the CR sample, has a face-centered cubic crystal structure with the lattice constant of 0.3644 nm, which is larger than the calculated lattice parameter using Vegard's law ($a=0.3636$), assuming all Ag was in solid solution, by 0.22%. After 2 h of aging (CR+HT2h), the Ag (111) peak appeared at 38.147°, which was not in good agreement with pure Ag (2θ at 38.318°). The small and broad Ag peaks revealed the low volume fraction and small size of the Ag precipitates in the Cu matrix. The intensity of the Ag peaks shown in Figure 2 can be ascribed to the longer aging time, and the higher amount of Ag precipitates present in

the Cu matrix that would have been received. Furthermore, Figure 2 shows an increase of the Cu₂O(111) peak intensity at ~29.5° 2θ with an increasing aging time. With a longer aging time, the sharper full width half maximum of the Cu₂O peaks can be seen. This could suggest that the copper favors the growth of the Cu₂O phase against the CuO. The difference of the height ratios between the Cu and Ag peaks resulted from the difference in the rolling textures. At 430°C aging temperature, the dislocations formed during plastic deformation would be annihilated through thermal treating. The XRD pattern (Figure 2) shows that the crystallize sizes of the samples also have been changed after aging. For example, the peak broadening at Cu(311) of the CR sample can be detected. The peak broadening phenomenon indicates that the lattice strain and the crystallite size variations were introduced during the cold rolling process. However, it can be clearly seen that there are peak splits at Cu(311) after aging for 2 and 18 h. The peak splits are due to the presence of the CuKα1 and CuKα2 radiations. This effect shows that the sample has a large crystal size. The stored energy accumulated during cold deformation and released by the re-distribution of dislocations at high temperature, which results in the grain or substructure sizes of plastically deformed CuAgZr alloy, can be

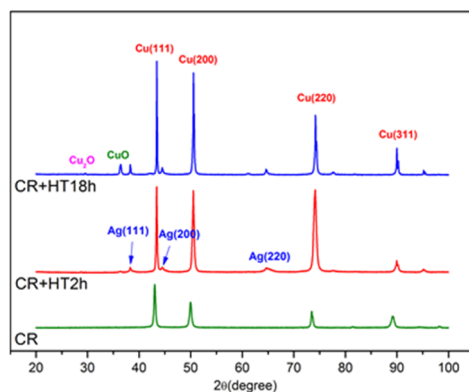


Figure 2. XRD patterns of the deformed Cu-7wt%Ag-0.05wt%Zr followed by isothermal aging at 430°C with various times

significantly changed during thermal treatment.

Electron Microscopy for Microstructural Investigation

Microstructures of CuAgZr alloy with and without plastic deformation prior to aging at 430°C for 18 h were investigated by secondary electron images (SEI). Figure 3 shows the microstructure of the aged CuAgZr alloy without being plastically deformed. It can be seen that there are 2 different types of Ag precipitation presented in the SEM micrographs, continuous precipitates and discontinuous precipitates. The continuous precipitates are thoroughly dispersed in the Cu matrix, as seen in area A of Figure 3(a). They grew along particular $\{111\}$ planes in the Cu matrix and could be clearly seen at high magnification (50kX), as shown in Figure 3(b). The cube-on-cube orientation relationship has been identified by the selected

area electron diffraction (SEAD) pattern from transmission electron microscopy in the previous work of Shizuya and Konno (2008). On the other hand, the growth of discontinuous precipitates is advancing from the grain boundary into the grain interior. Discontinuous precipitation is also known as cellular precipitation that nucleates at the grain boundary (area B of Figure 3(a)). Discontinuous precipitates originate from the grain boundary (dotted line in Figure 3(a)) and they carry the grain boundary along when growing (Porter *et al.*, 2009). It can be obviously seen that the discontinuous precipitates are considerably larger than the continuous precipitates. Microstructures of the 18-h thermal treatment of plastically deformed CuAgZr alloy are shown in Figure 4. The Ag particles are homogeneously dispersed in the Cu matrix without preferred directions and planes. There is no evidence of discontinuous precipitates growing from the grain boundary.

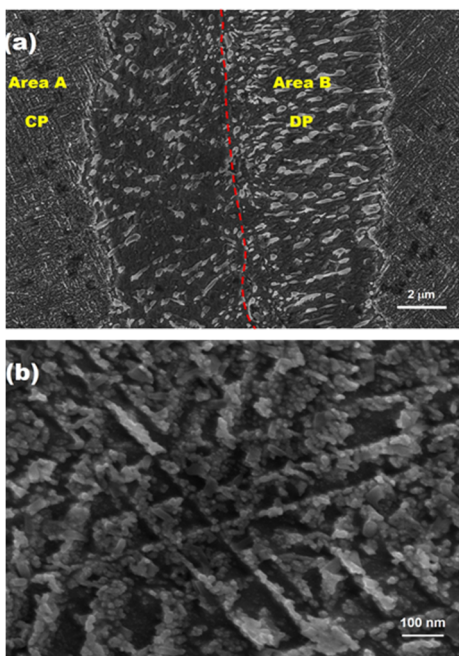


Figure 3. SEM micrographs of CuAgZr alloy without plastic deformation prior to aging at 430°C for 18 h: (a) 6000X and (b) 50000 X

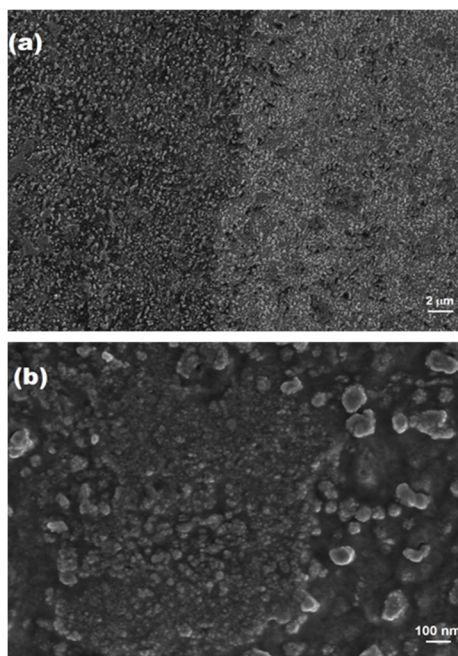


Figure 4. SEM micrographs of plastically deformed CuAgZr alloy followed by aging at 430°C for 18 h: (a) 3000 X and (b) 30000 X

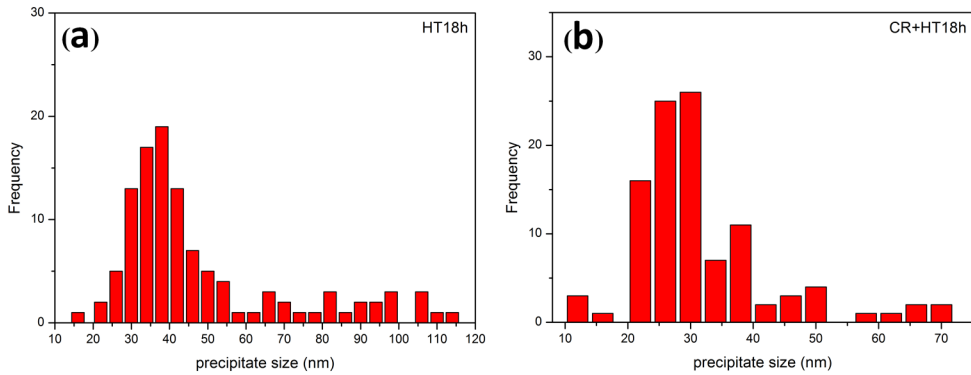


Figure 5. Histogram of Ag precipitates in CuAgZr alloy after aging at 430°C for 18 h: (a) non-deformed and (b) cold rolled

The average sizes of the Ag precipitates measured from the SEI are listed in Table 1. Histograms of the precipitate sizes are shown in Figures 5(a-b) indicating that the size of the Ag nano-particles are affected by plastic deformation prior to the thermal routine. The average size of the Ag particles appearing in the non-deformed samples is larger than the average size in the deformed samples by 35%. The disappearance of the discontinuous precipitates can be ascribed to a large increase in the number of nucleation sites as a result of plastic deformation (Porter *et al.*, 2009).

Table 1. The sizes of Ag precipitates in CuAgZr alloy after aging at 430°C for 2 and 18 h

Sample	Aging time (h)	Measured size from SEI (nm)
Non-deformed	2	36.96±12.13
	18	46.30±22.72
Cold rolled	2	21.85±3.56
	18	29.58±11.50

The free energy of the deformed samples is greater than that of the aged samples and approximately equal to the stored strain energy. The amount of stored energy can be increased by increasing the degree of deformation, lowering the deformation temperature, and altering the alloy

constituents. Phase transformation proceeds by a process of nucleation and growth to decrease the free energy of the system. This can indicate that cold working decreases the size of the Ag precipitates by introducing more nucleation sites in the Cu matrix.

Figure 6 shows transmission electron micrographs of a cold rolled sample followed by isothermal heat treatment at 430°C for 2 h. It can be seen that the darker contrast of tiny spots are Ag particles. The Ag precipitates are homogeneously distributed through Cu parent grains. The average size of the Ag precipitates (approximately 20 nm) measured from the TEM micrograph is close to the measured size from the SEM investigation. The SEAD pattern taken from $[0\bar{1}\bar{1}]$ zone axis in Figure 6(b) shows that the Ag precipitates and Cu matrix have a particular orientation relationship (OR). The cube-on-cube OR can be described as follows:

$$[110]_{\text{Cu}} // [110]_{\text{Ag}} \text{ and } (010)_{\text{Cu}} // (010)_{\text{Ag}}$$

From the SEAD pattern, it can be clearly seen that there is a specific orientation relationship between the Ag particles and Cu matrix. However, the Ag particles in the deformed samples have not aligned themselves onto certain planes and directions, as shown in the non-deformed samples seen in previous works (Räty and Miekko-Oja, 1968; Piyawit *et al.*, 2014). This phenomenon can also be

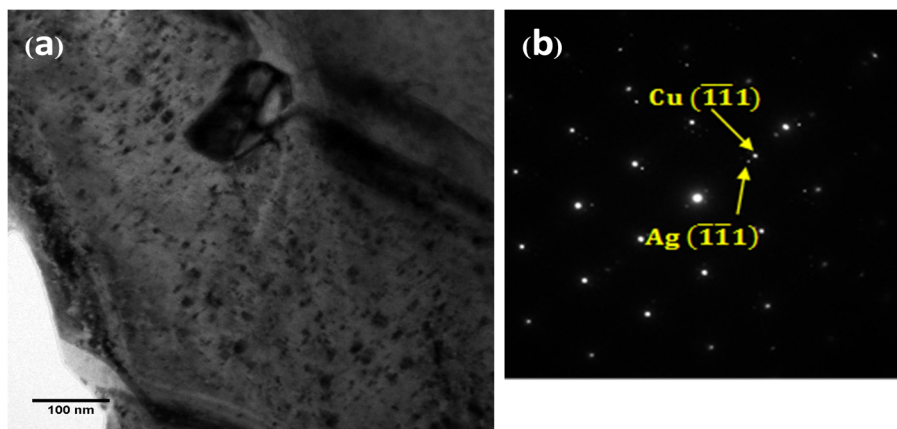


Figure 6. TEM micrographs of cold rolled (CR) CuAgZr alloy after aging at 430°C for 2 h: (a) bright field image and (b) SEAD pattern

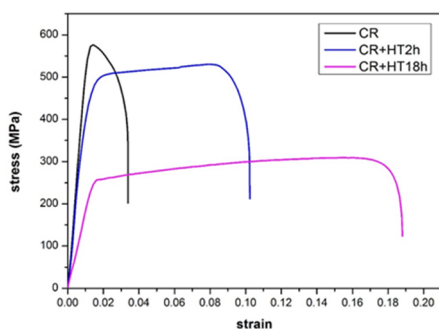


Figure 7. Typical stress-strain curve of cold rolled CuAgZr alloys at 90% reduction thickness following different thermal routines

directly observed under SEM, in which the Ag precipitates are thoroughly dispersed in the Cu matrix.

Comparisons of Mechanical Properties and Electrical Conductivity

Selected autographic stress-strain curves obtained on some specimens from the cold-drawn and aged Cu-7wt%Ag-0.05wtZr alloy are reproduced in Figure 7, as illustrative of the different types of flow observed in the tension tests. It can be seen that the aged

samples exhibit strain hardening behavior after yielding. This is due to the low stacking fault energy of copper. The strength, ductility, and electrical conductivity of CuAgZr are listed in Table 2. It can be seen that the properties of the rolled samples followed by aging have significantly changed. Especially, the ductility has been improved observably. Electrical conductivities of the materials are compared to the resistivity of annealed pure copper which is 1.724×10^{-8} ohm \cdot m. This number is conferred to 100% IACS (International Annealed Copper Standard). The electrical conductivity of plastically deformed CuAgZr alloy with the 2.3 logarithmic strain is approximately at 45% of the annealed pure copper. However, it has a superior strength of more than 2.5 times that of pure copper. There are the direct effects of work hardening and the increase of the dislocation density in the Cu lattice. The alloy, after 2 h of aging, retains its high strength without sacrificing the ability of the electrical conductive materials. From Figure 7, the mechanical strength of the 18-h aged samples has significantly dropped with an extensive amount of deformation before fracture.

The fracture morphology of the tensile tested samples examined under SEM is shown in Figure 8. A dimple formation can be seen on

Table 2. Mechanical properties and electrical conductivity of CuAgZr alloy

Sample	Yield strength (Mpa)	Ultimate tensile strength (Mpa)	%Elongation	%IACS
90% RT rolled	544	573	3.39%	46.74%±1.47
90% RT + 430 C, 2 h	434	529	10.22%	70.38±1.66
90% RT + 430 C, 18 h	254	307	18.83%	84.67±1.37

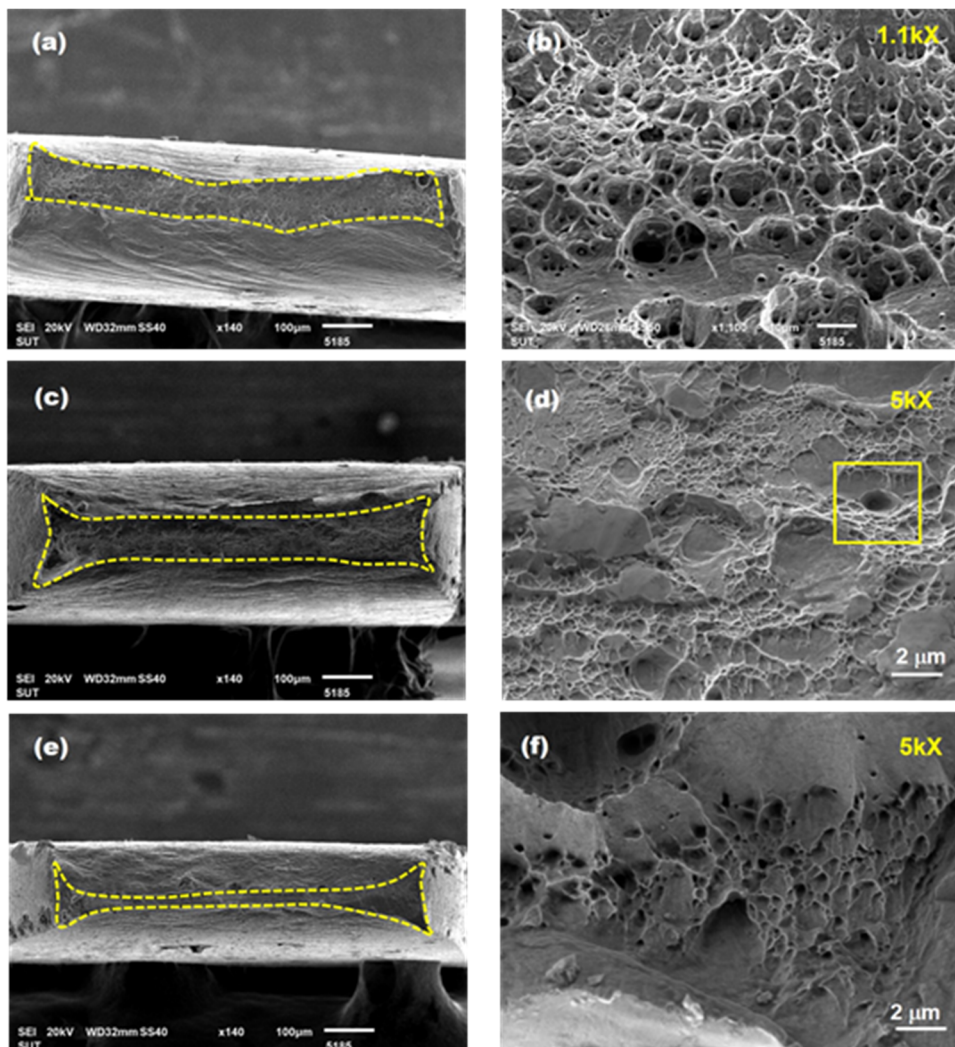


Figure 8. Secondary electron images of tensile specimens' fracture surfaces: (a and b) as-rolled (CR), (c and d) CR+HT2 h, and (e and f) CR+HT18 h

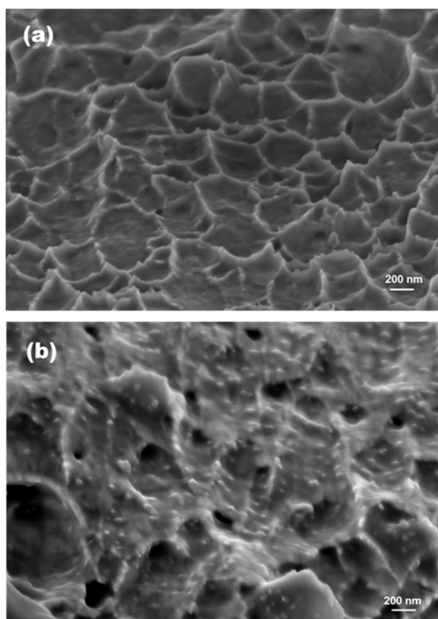


Figure 9. Secondary electron micrographs of tensile fracture surfaces at 30 kX: (a) CR+HT2 h and (b) CR+HT18 h

the fracture surfaces. This suggests that the CuAgZr alloy has a ductile fracture behavior. The depth of these dimples can be attributed to the ductility of each sample. The high strength of the as-rolled sample has a comparatively small reduction in area, as seen in Figure 8(a) compared to the more ductile samples shown in Figure 8 (c and e). CR+HT2h shows a good combination of strength and deformability, as shown in the stress-strain curves (Figure 7). There are plenty of shallow dimples found at the fracture surface (Figure 8(d) and Figure 9(a)). Dimples are characteristic of micro-void coalescence, which is a ductile form of fracture. Small particles at the bottom of the crater (the square area in Figure 8(d)) were the origins of the voids and the particles acted as stress concentrations. The dimples' sizes are ranged from nanometers to sub-micron. The 18-hours aged sample (Figures 8 (e and f)) has relatively deeper dimples than the as-rolled and 2-h aged sample. The high reduction area (the dotted area in Figure 8(e)) of CR+HT18h corresponds to the mechanical behavior that

showed good deformability. The over-aging phenomenon would take approximately a 50% part of the decrease of the strength. It can obviously be seen in the SEM image (Figure 9(b)) that there are coarser Ag precipitates present at the fracture surface.

Conclusions

Characterizations of plastically deformed Cu-7wt%Ag-0.05wt%Zr with the logarithmic strain of 2.3 were carried out by using XRD analysis and electron microscopy. The XRD and SEM results were in good agreement with the presence of Ag particles found in the Cu matrix after heat treatments. The XRD results showed the formation of Ag precipitates after the aging treatment. The shift of the main Cu peaks in the deformed solution-treated samples confirmed the introduction of Ag in the lattice of the Cu matrix. The amount of Ag present after the aging treatment was increased with the increased aging time. This was in good agreement with the electron microscopy analysis that the coarsening of the Ag precipitates was likely to be due to the Ostwald ripening. Plastic deformation introduced more nucleation sites to the Cu matrix microstructure resulting in finer Ag precipitated particles homogeneously dispersed in the Cu matrix. Tailoring the Ag nanoparticle microstructure through the aging process would give rise to the desired combination of good strength and electrical conductivity.

Acknowledgments

This work was financially supported by Suranaree University of Technology under grant No. SUT7-713-58-12-65.

References

- Bao, G., Xu, Y., Huang, L., Lu, X., Zhang, L., Fang, Y., Meng, L., and Liu, J. (2016). Strengthening effect of Ag precipitates in Cu-Ag alloys: a quantitative approach. *Mat. Res. Lett.*, 4(1):37-42.
- Bowler, N. and Huang, Y. (2005). Electrical conductivity measurement of metal plates using broadband

- eddy-current and four-point methods. *Meas. Sci. Technol.*, 16(11):2193-2200.
- Gaganov, A., Freudenberger, J., Botcharova, E., and Schultz, L. (2006). Effect of Zr additions on the microstructure, and the mechanical and electrical properties of Cu-7 wt.%Ag alloys. *Mat. Sci. Eng. A-Struct.*, 437(2):313-322.
- Hanama, D., Hachouf, M., Bouzama, L., and Biskri, Z.E.A. (2011). Precipitation kinetic and mechanism in Cu-7wt%Ag alloy. *Materials Sciences and Application*, 2(7):899-910.
- Hirota, T., Imai, A., Kumano, T., Ichihara, M., Sakai, Y., Inoue, K., and Maeda, H. (1994). Development of Cu-Ag alloys conductor for high field magnet. *IEEE T. Magn.*, 30(4):1891-1894.
- Lyubimova, J., Freudenberger, J., Gaganov, A., Klauß, H., and Schultz, L. (2010). Strain enhanced high strength Cu–Ag–Zr conductors. *Mater. Sci. Forum*, 633-634:707-715.
- Monzen, R., Terazawa, T., and Watanabe, C. (2010). Influence of external stress on discontinuous precipitation behavior in a Cu-Ag alloy. *Metall. Mater. Trans. A*, 41A:1936-1941.
- Piyawit, W. (2014). Effect of processing scheme on precipitation mechanisms and evolution of microstructures and properties of CuAgZr alloy. [Ph.D. thesis]. Department of Materials Science and Engineering, College of Engineering, North Carolina State University, Raleigh, NC, USA, 129p.
- Piyawit, W., Xu, W.Z., Mathaudhu, S.N., Freudenberger, J., Rigsbee, J.M., and Zhu, Y.T. (2014). Nucleation and growth mechanism of Ag precipitates in a CuAgZr alloy. *Mat. Sci. Eng. A-Struct.*, 610:85-90.
- Porter, D.A., Easterling, K.E., and Sherif, M.Y. (2009). *Phase Transformation in Metals and Alloys*. 3rd ed. CRC Press, Boca Raton, FL, USA, 500p.
- Räty, R. and Miekko-Oja, H.M. (1968). Precipitation associated with the growth of stacking faults in copper-silver alloys. *Philos. Mag.*, 18(156):1105-1125.
- Shizuya, E. and Konno, T.J. (2008). A study on age hardening in Cu-Ag alloys by transmission electron microscopy. In: Fujikawa, Y., Nakajima, K., and Sakurai, T. (eds). *Frontiers in Materials Research*. 10:217-226.